RSC Advances

PAPER

View Article Online
View Journal | View Issue

Cite this: *RSC Adv.*, 2017, **7**, 10922

Near-infrared probes based on fluorinated Si-rhodamine for live cell imaging†

Suxia Shen,[a] Jingru Yu,[a] Yaomin Lu,[a] Shuchen Zhang,[b] Xuegang Yi[a] and Baoxiang Gao*[ab]

Received 20th December 2016
Accepted 3rd February 2017

DOI: 10.1039/c6ra28455h

rsc.li/rsc-advances

The syntheses and biological applications of three Si-rhodamine probes with substituent groups on the pendant phenyl ring are reported. In solution, these Si-rhodamine probes (**AZSiR**) show slight aggregation. By introducing a methyl group at the 2-position of the pendant phenyl ring, the **AZSiR-2** probe shows almost unchanged absorption and emission peaks, and a three times higher fluorescence quantum yield than that of **AZSiR-1**. However, the photostability of the **AZSiR-2** probe becomes poor. By changing the substituent groups from methyl to trifluoromethyl, the **AZSiR-3** probe displays slightly red-shifted absorption and emission peaks, and good photostability. Furthermore, the bulky groups on the phenyl ring of Si-rhodamine prevent nucleophilic attack through steric hindrance, and endow Si-rhodamine probes good chemical stability in nucleophilic systems. These Si-rhodamine probes have excellent live cell permeability and low cytotoxicity. Importantly, the Si-rhodamine probe with trifluoromethyl at the 2-position of the pendant phenyl ring retains high brightness and excellent stability even in a harsh physiological environment.

Introduction

Rhodamines are well-known fluorescent dyes that display water solubility, high fluorescence quantum yields and high molar extinction coefficients,[1,2] and they are widely utilized in various fluorescent probes for bioimaging.[3–5] However, these dyes basically have green to red fluorescence. Near-infrared (NIR) (650–900 nm) fluorescence dyes are attractive for biological applications because of minimum photo-damage to biological samples, deep tissue penetration, and minimum interference from background auto-fluorescence in the living systems.[6,7] Recently, a new class of NIR silicon-substituted rhodamines, in which the O atom at the 10-position of the xanthene moiety is replaced with a SiMe2 group, have been developed for fluorescence bioimaging.[8–10]

Latestly, Lavis replaced these dimethyl amino groups of the classic tetramethylrhodamine with four-membered azetidines, and created so called Janelia Fluor (JF) dyes.[11] This is a minor change in structure but causes a large increase in brightness and photostability. However, these fluorescent rhodamines are cationic conjugated compounds, and the nucleophilic attack on the 9th carbon atom of the xanthene ring of these rhodamine derivatives would occur easily, and induce drastic changes in optical properties.[12,13] Thus, the Si-rhodamine probes with high stability are highly desired for practical images *in vivo*. Here, we report the NIR Si-rhodamine probes (**AZSiR**) with the bulky groups on benzene at 9-position of the xanthene moiety (Chart 1). The **AZSiR** probes possess high fluorescence quantum yields, improved stability in the nucleophilic biology system.

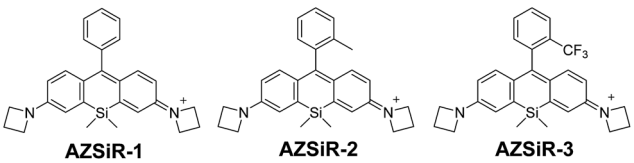

Chart 1 Chemical structures of **AZSiR** probes.

Results and discussion

The **AZSiR** probes were synthesized according to Scheme 1. 3,6-Dihydroxy-Si-xanthone (1) was obtained according to literature procedures.[8] Triflation of 3,6-dihydroxy-Si-xanthone (1) afforded compound ditriflate-Si-xanthone (2). Then the important intermediate of diazetidine-Si-xanthone (3) was synthesized by compound 2 and azetidine under the catalysis of Pd_2dba_3 and XPhos. The azetidinyl-Si-rhodamines were synthesized by nucleophilic addition of the various kinds of freshly prepared appropriate benzene lithium solution to the diazetidine-Si-xanthone.

[a]*Key Laboratory of Medicinal Chemistry and Molecular Diagnosis (Hebei University), Ministry of Education, Baoding, 071002, China*

[b]*Key Laboratory of Analytical Science and Technology of Hebei Province, College of Chemistry and Environmental Science, Hebei University, Baoding, 071002, China. E-mail: bxgao@hbu.edu.cn; Fax: +86 3125077374*

† Electronic supplementary information (ESI) available. See DOI: 10.1039/c6ra28455h

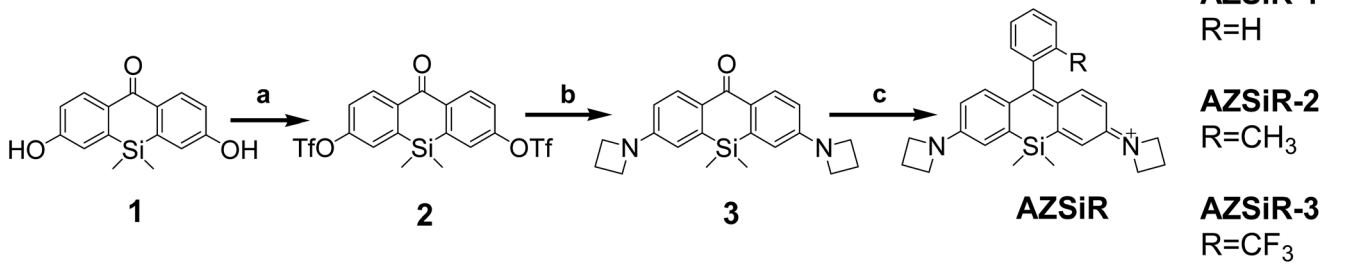

Scheme 1 Reagents and conditions: (a) 3,6-dihydroxy-Si-xanthone, CH_2Cl_2, 0 °C, pyridine, trifluoromethanesulfonic anhydride, room temperature, 2 h. (b) Compound 1, azetidine, Pd_2dba_3, XPhOS, Cs_2CO_3, 1,4-dioxane, 100 °C, 4 h. (c) Appropriate bromobenzene, *tert*-butyllithium (1.3 M), 2-methyltetrahydrofuran −116 °C, −116 °C to rt, 2 N HCl aq.

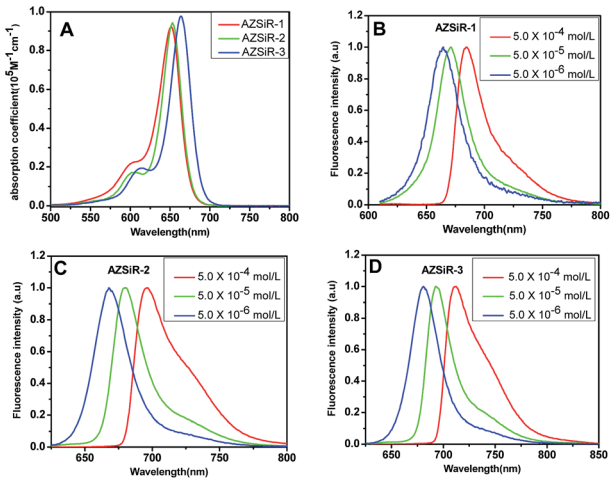

Fig. 1 UV-Vis absorption spectroscopy and concentration-dependent of AZSiR in dichloromethane solution. (A) UV-Vis absorption spectroscopy of AZSiR probes; (B) AZSiR-1; (C) AZSiR-2; (D) AZSiR-3.

Table 1 Spectroscopic data for the AZSiR probes

	$\lambda_{abs}{}^a$ [nm]	ε^a [mol L^{-1} cm^{-1}]	$\lambda_{em}{}^a$ [nm]	Φ^a [%]	Φ^b [%]
AZSiR-1	652	92 000	663	24	19
AZSiR-2	653	94 000	667	76	57
AZSiR-3	664	98 000	681	74	54

[a] Measured in dichloromethane with a concentration of 10^{-5} mol L^{-1}. [b] Measured in PBS + 1% DMSO with a concentration of 10^{-5} mol L^{-1}.

These **AZSiR** probes were fully characterized by H-NMR spectroscopy, C-NMR spectroscopy, and mass spectrometry, which can be found in the ESI.† These **AZSiR** probes show water solubility, and high solubility in common organic solvents such as dichloromethane, tetrahydrofuran, dimethyl sulfoxide. The UV-Vis absorption spectroscopy and fluorescence spectroscopy of the **AZSiR** probes in dichloromethane are shown in Fig. 1, and the photophysical data are summarized in Table 1.

In dichloromethane solution, **AZSiR-1** exhibited NIR absorption and emission with maxima at $\lambda_{abs} = 652$ nm and $\lambda_{em} = 663$ nm respectively. Introducing 2-methyl group on the pendant phenyl ring, **AZSiR-2** showed almost same absorption maxima ($\lambda_{abs} = 653$ nm) and emission maxima ($\lambda_{em} = 667$ nm). Compared with those of **AZSiR-2**, **AZSiR-3** with trifluoromethyl substituent displayed slight red-shifted absorption and emission maxima ($\lambda_{abs} = 664$ nm and $\lambda_{em} = 681$ nm). The bathochromic electronic transitions observed for **AZSiR-3** predominantly arises from a stabilization of the LUMO by the electron-withdrawing trifluoromethyl substituent.[14] **AZSiR-1** showed relatively low fluorescence quantum yield (24%). In contrast, the fluorescence quantum yield of **AZSiR-2** was significantly increased to 76% by introducing a stopper 2-methyl group on the phenyl ring, which can maintain an orthogonal relationship between the benzene moiety and the fluorophore, and reduce the energy loss by restricting rotation.[15] Furthermore, **AZSiR-3** with trifluoromethyl groups also maintained a high fluorescence quantum yield (74%).

The optical properties of **AZSiR** probes in dichloromethane solution were furthermore investigated *via* concentration-dependent steady state and transient state fluorescence spectroscopy (Fig. 1 and S2†). When the solution concentration increased from 5.0×10^{-6} to 5.0×10^{-4} mol L^{-1}, the absorption peaks and extinction coefficient of **AZSiR** probes did not change. However, within the same concentration range, the emission maximum peaks were continuously red-shifted by 21 nm (**AZSiR-1**: from 663 to 684 nm), 26 nm (**AZSiR-2**: from 670 to 696 nm), and 31 nm (**AZSiR-3**: from 681 to 712 nm). These results suggest that **AZSiR** probes have slight aggregation in dichloromethane solution.[16] To further demonstrate the aggregation behavior of **AZSiR** probes, time resolved fluorescence measurements were performed. The curves of the fluorescence decays for three **AZSiR** probes were prolonged in the concentration range from 5.0×10^{-6} to 5.0×10^{-4} mol L^{-1} (Fig. S2†). The prolonged lifetimes upon increasing concentration are attributed to the monomer transfer to aggregates.[17] These **AZSiR** probes showed good solubility in PBS, which is important for probes used in biology system.[18] Furthermore, the fluorescence quantum yields of **AZSiR** probes with bulky groups on 2-position of the pendant phenyl ring (**AZSiR-1** and **AZSiR-2**) in PBS solution were lower than those in organic solution but still remained high (54–57%).

In order to compare the photostability of **AZSiR** probes reported here with fluorophores commonly used NIR probes, the

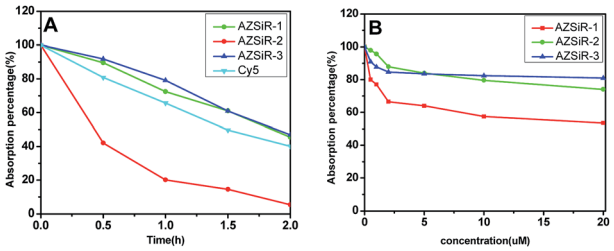

Fig. 2 Photostability and chemostability of 10 μM **AZSiR** probes in dichloromethane solution. (A) Time-dependent absorption of **AZSiR** probes under continuous irradiation with 660 nm LED laser. (B) Absorption of **AZSiR** probes with different concentration cysteine.

photobleaching measurements of **AZSiR** probes, and Cy5 were performed under continuous irradiation with 660 nm LED laser (Fig. 2A). After irradiation for 30 min, 80% absorption intensity of Cy5 persisted, **AZSiR-1** and **AZSiR-3** kept 94% absorption intensity. However, same photobleaching experiments revealed that only 43% absorption intensity of **AZSiR-2** remained. It is worth noting that the absorption maxima of **AZSiR-2** shifted from 652 nm to 618 nm during 2 h continuous irradiation. The chemical inertness of trifluoromethyl on phenyl ring of Si-rhodamine should be responsible for good photostability of **AZSiR-3**. In live cells, the molecules containing cysteine are abundant, these molecules with thiol can act as nucleophiles to react with **AZSiR** probes. To test the stability of **AZSiR** probes under nucleophilic condition, changes in absorbance were monitored upon addition of cysteine. As shown in Fig. 2B, only slight decreases of absorption of **AZSiR-2** and **AZSiR-3** were observed when the concentration of cysteine was 0.5 μM, whereas the absorption of **AZSiR-1** dropped to 80%. Increasing the concentration of cysteine from 0.5 μM to 20 μM, only 53% absorption of **AZSiR-1** remained. In contrast, **AZSiR-3** retained 81% of its initial absorption. It could be that the bulky substituents on phenyl ring of Si-rhodamine prevent the nucleophilic attack of cysteine through steric hindrance.[9b,19] These results indicate the trifluoromethyl groups on 2-position of phenyl ring are beneficial to improve the fluorescence quantum yields and stability of the Si-rhodamine probes.

To demonstrate the potential utility of **AZSiR** probes for cellular imaging, their cytotoxicity was assessed using MTT cell-viability assays. These **AZSiR** probes showed over 85% cell viability under 10 μM within 24 h of incubation time (Fig. S6†), indicated that **AZSiR** probes have low cytotoxicity. To evaluate the feasibility of imaging in living cells using **AZSiR** probes, they were employed to stain HeLa cells for the CLSM images (Fig. 3). Some fluorescent dots were observed in the cells stained **AZSiR** probes, indicating that **AZSiR** probes have good cell-membrane permeability. The quantified fluorescence intensities of multi-points in cells stained with **AZSiR-1**, **AZSiR-2** and **AZSiR-3** were shown in Fig. 3C, F and I. The mean fluorescence intensities from the cells stained with **AZSiR-2** and **AZSiR-3** were twice higher than that of the cells stained with **AZSiR-1**. The intracellular photostability of **AZSiR** probes under CLSM imaging conditions was investigated by continuous laser scanning (Fig. 4). The intracellular intensity of the **AZSiR-3** fluorescence

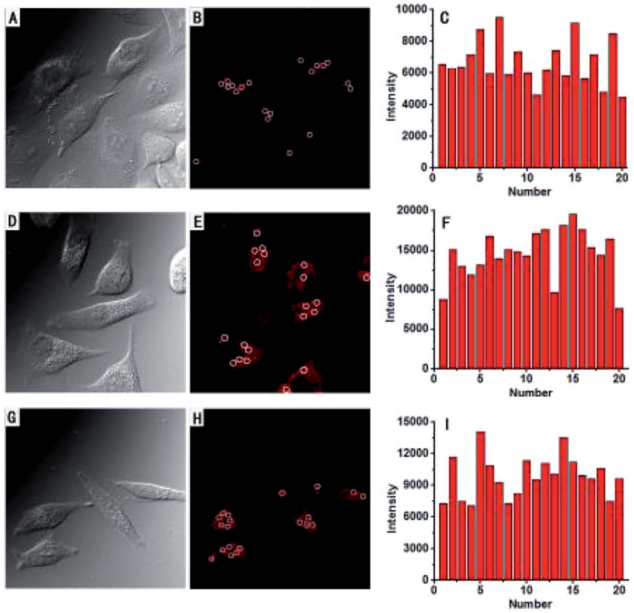

Fig. 3 Confocal microscopy images and mean fluorescence intensities of HeLa cells incubated with **AZSiR** (5 μM) at 37 °C for 30 min: the bright-field ((A) **AZSiR-1**; (D) **AZSiR-2**; (G) **AZSiR-3**), confocal fluorescence images ((B) **AZSiR-1**; (E) **AZSiR-2**; (H) **AZSiR-3**) and mean fluorescence intensities of multi-points in cells ((C) **AZSiR-1**; (F) **AZSiR-2**; (I) **AZSiR-3**).

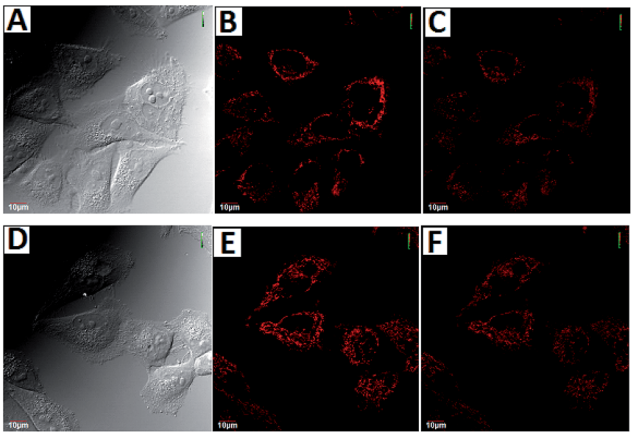

Fig. 4 The photostability assays of HeLa cells incubated with **AZSiR** (5 μM) at 37 °C for 30 min. The continuous laser scanning confocal images of HeLa cells stained with **AZSiR-2** ((A) bright field; (B) first frame; (C) 20th frame), **AZSiR-3** ((D) bright field; (E) first frame; (F) 20th frame).

signal remained almost unchanged even after scanning 20 images using identical laser intensities (Fig. 4F), whereas a significant decrease in signal intensity was detected for the cells stained with **AZSiR-2** during the measurement (Fig. 4C).

Conclusions

In summary, we designed new Si-rhodamine probes with different substituent groups. The bulky methyl groups on 2-

position of the pendant phenyl ring are beneficial to improve fluorescence quantum yield, and prevent the nucleophilic attack for good chemical stability. Furthermore, the chemical inertness of trifluoromethyl groups endow Si-rhodamine probes better photostability. High fluorescence quantum yields, good photo-chemistry stability, live cell permeability, and low cytotoxicity make the fluorinated Si-rhodamine dyes excellent probes for live-cell imaging.

Experimental

Materials and instrumentation

All the chemicals used in synthesis are analytical pure and were used as received. UV/Vis spectra were recorded on a Shimadzu WV-2550 spectrophotometer. Fluorescence spectra were recorded on a Shimadzu RF-5301 fluorescence spectrophotometer. The H-NMR spectra and C-NMR spectra were recorded at 20 °C on 600 MHz or 150 MHz NMR spectrometer (Bruker). Mass spectra were carried out with Agilent LC/MSD XCT Trap. CLSM images were obtained using Olympus confocal laser scanning microscopy (Olympus Fluoview 1000). The fluorescence lifetimes were recorded on an Edinburgh Analytical Instruments FLS980 spectrometer, equipped with a supercontinuum ultrafast fiber lasers (Fianium), using the time correlated single photon-counting (TCSPC) method. Typically, 10 000 counts were collected at the peak channel, and the decay curves were fitted by least-squares deconvolution with original Edinburgh Instrument software; the quality of the parameters were judged by the reduced χ^2 values and the randomness of the weighted residuals. The instrument used for HPLC analysis is Shimadzu LC-6AD high performance liquid chromatography, and the eluent were A (water : acetonitrile, v/v = 90 : 10) and B (acetonitrile : water, v/v = 90 : 10).

Synthetic procedures

3,6-Ditriflate-Si-xanthone (2). Compound 1 (300 mg, 1.11 mmol) was suspended in 10 mL of anhydrous CH_2Cl_2, and the solution was stirred at 0 °C. Pyridine (1.44 mL, 17.76 mmol, 16 eq.) was added and stirred uniformly. Triflic anhydride (1.50 mL, 8.88 mmol, 8 eq.) were added dropwise, and stirred at room temperature for 2 h. It was subsequently diluted with water and extracted with dichloromethane. The combined organic phase was washed with water and brine, dried over Na_2SO_4, filtered and evaporated. The resultant residue was quickly purified by silica gel chromatography (AcOEt/hexane, 4 : 3, v/v) yielded 539 mg (1.01 mmol, 91%) of pure product 2 as a colorless solid. ^{1}H-NMR (600 MHz, $CDCl_3$); δ 8.33 (d, J = 8.4 Hz, 2H), 7.99 (d, J = 2.4 Hz, 2H), 7.66–7.64 (dd, J = 2.49 Hz, 2H), 0.46 (s, 6H); ^{13}C-NMR (150 MHz, $CDCl_3$): δ 154.0, 145.0, 141.9, 134.7, 128.7, 125.7.

3,6-Diazetidine-Si-xanthone (3). In a glove box filled with dry nitrogen, compound 2 (500 mg, 0.936 mmol), Pd_2dba_3 (86.4 mg, 0.0936 mmol, 0.1 eq.), XPhOS (134.4 mg, 0.282 mmol, 0.3 eq.), and Cs_2CO_3 (856 mg, 2.63 mmol, 2.8 eq.) were mixed. A suspension of azetidine (152 μL, 2.25 mmol, 2.4 eq.) in anhydrous dioxane (8 mL) was added dropwise and stirred at 100 °C for 4 h. It was then the reaction mixture was cooled to room temperature, diluted with dichloromethane. The combined organic phase was washed with water and brine, dried over Na_2SO_4, filtered and evaporated. Purification by silica gel chromatography (EtOAc/hexanes, 1 : 5, v/v) afforded compound 3 (326.2 mg, 0.786 mmol, 84%) as an pale yellow solid. ^{1}H-NMR (600 MHz, $CDCl_3$) δ 8.29 (d, J = 9 Hz, 2H), 6.54–6.43 (dd, J = 2.4, 8.4 Hz, 2H), 6.40 (d, J = 2.4 Hz, 2H), 3.95 (t, J = 7.8 Hz, 8H), 2.38–2.33 (m, 4H), 0.36 (s, 6H); ^{13}C-NMR (150 MHz, $CDCl_3$): δ 153.7, 141.5, 132.6, 131.5, 114.2, 113.2, 52.8, 17.8; MS (ESI): calcd for: $C_{21}H_{24}N_2OSi$ m/z = 348.1, found: 349.3 $[M + H]^+$.

AZSiR-1. In a nitrogen-flushed flask fitted with a septem cap, bromobenzene (224.5 mg, 1.43 mmol, 10 eq.) was dissolved in anhydrous 2-methyltetrahydrofuran (10 mL) and the solution was cooled to −116 °C, *tert*-BuLi (1.1 mL, 1.43 mmol, 10 eq.) was slowly added dropwise, and the mixture was stirred at the same for 20 minutes. Compound 3 (50 mg, 0.143 mmol, 1 eq.) in dry 2-methyltetrahydrofuran (5 mL) was slowly added dropwise *via* a syringe at −116 °C. Stirring was continued for 20 minutes, then the solution was warmed to room temperature, further stirred for 2 h, quenched with 2 N HCl aq., and basified with sat. $NaHCO_3$ aq. The aqueous solution was extracted with dichloromethane, and the combined organic phase was washed with water and brine, dried over Na_2SO_4, filtered and evaporated. The resultant residue was quickly purified by HPLC (eluent: A/B = 90/10 to 10/90, 40 min) to afford **AZSiR-1** (20.5 mg, 35% yield) as blue solid. ^{1}H-NMR (600 MHz, $CDCl_3$): δ 7.47–7.46 (m, 3H), 7.17–7.15 (m, 2H), 7.00 (d, J = 9 Hz), 6.84 (d, J = 2.4 Hz, 2H), 6.22 (q, J = 2.4, 9 Hz, 2H), 4.40 (s, 8H), 2.60 (m, 4H), 0.57 (s, 6H); ^{13}C-NMR (150 MHz, $CDCl_3$): δ 168.9, 153.5, 148.5, 142.4, 140.1, 129.9, 129.2, 128.9, 128.5, 120.0, 112.4, 53.1, 52.5, 30.4, 30.1, 30.0, 17.0, 1.8, −0.2. MS (ESI): calcd for: $C_{27}H_{29}N_2Si^+$ m/z = 409.2, found: 409.2 $[M]^+$.

AZSiR-2. In a nitrogen-flushed flask fitted with a septem cap, 2-bromotoluene (244.6 mg, 1.43 mmol, 10 eq.) was dissolved in anhydrous 2-methyltetrahydrofuran (10 mL) and the solution was cooled to −116 °C, *tert*-BuLi (1.1 mL, 1.43 mmol, 10 eq.) was slowly added dropwise, and the mixture was stirred at the same for 20 minutes. Compound 3 (50 mg, 0.143 mmol, 1 eq.) in dry 2-methyltetrahydrofuran (5 mL) was slowly added dropwise *via* a syringe at −116 °C. Stirring was continued for 20 minutes, then the solution was warmed to room temperature, further stirred for 2 h, quenched with 2 N HCl aq., and basified with sat. $NaHCO_3$ aq. The aqueous solution was extracted with dichloromethane, and the combined organic phase was washed with water and brine, dried over Na_2SO_4, filtered and evaporated. The resultant residue was quickly purified by HPLC (eluent: A/B = 70/30 to 10/90, 50 min) to afford **AZSiR-2** (22.9 mg, 38% yield) as blue solid. ^{1}H-NMR (600 MHz, $CDCl_3$): δ 7.35 (t, J = 7.2, 7.2 Hz, 1H), 7.26 (t, J = 8.4, 7.8 Hz, 2H), 7.00 (d, J = 7.8 Hz, 2H), 6.92 (d, J = 9.6 Hz, 2H), 6.77 (d, J = 2.4 Hz, 2H), 6.19 (q, J = 2.4, 2.4 Hz, 2H), 4.35 (s, 8H), 2.58–2.52 (m, 4H), 1.94 (s, 3H), 0.54 (d, J = 2.4, 2.4 Hz, 6H). ^{13}C-NMR (150 MHz, $CDCl_3$): δ 168.1, 151.9, 147.0, 140.1, 129.2, 127.9, 127.8, 126.5, 124.6, 118.1, 110.9, 51.2, 28.7, 28.5, 28.3, 26.2, 21.7, 18.3, 15.1, 13.1, −1.8, −2.1. MS (ESI): calcd for: $C_{28}H_{31}N_2Si^+$ m/z = 423.2, found: 423.2 $[M]^+$.

AZSiR-3. In a nitrogen-flushed flask fitted with a septem cap, 2-bromobenzotrifluoride (321.8 mg, 1.43 mmol, 10 eq.) was dissolved in anhydrous 2-methyltetrahydrofuran (10 mL) and the solution was cooled to −116 °C, *tert*-BuLi (2.2 mL, 2.86 mmol, 20 eq.) was slowly added dropwise, and the mixture was stirred at the same for 20 minutes. Compound 3 (50 mg, 0.143 mmol, 1 eq.) in dry 2-methyltetrahydrofuran (5 mL) was slowly added dropwise *via* a syringe at −116 °C. Stirring was continued for 20 minutes, then the solution was warmed to room temperature, further stirred for 2 h, quenched with 2 N HCl aq., and basified with sat. $NaHCO_3$ aq. The aqueous solution was extracted with dichloromethane, and the combined organic phase was washed with water and brine, dried over Na_2SO_4, filtered and evaporated. The resultant residue was quickly purified by HPLC (eluent: A/B = 70/30 to 10/90, 50 min) to afford **AZSiR-3** (19 mg, 28% yield) as blue solid. ^{1}H-NMR (600 MHz, $CDCl_3$): δ 7.78 (d, J = 7.8 Hz, 2H), 7.69–7.61 (m, 2H), 7.22 (t, J = 7.2, 7.2 Hz, 1H), 6.79 (q, J = 1.8, 9.6 Hz, 4H), 6.22 (q, J = 1.8, 2.4 Hz), 4.39 (s, 8H), 2.58–2.56 (m, 4H), 0.61 (s, 3H), 0.47 (s, 3H). ^{13}C-NMR (150 MHz, $CDCl_3$): δ 163.4, 151.7, 146.8, 140.1, 136.3, 130.8, 130.1, 128.2, 126.8, 125.6, 118.2, 110.8, 51.3, 30.9, 28.7, 21.7, 15.1, 13.1, −1.3, −2.9. MS (ESI): calcd for: $C_{28}H_{28}F_3N_2Si^+$ m/z = 477.2, found: 477.3 $[M]^+$.

Cell culture and imaging

HeLa cells were cultured in Dulbecco's modified Eagle's medium (high glucose), supplemented with 10% (v/v) fetal bovine serum, penicillin (100 units per mL) and streptomycin (100 μg mL^{-1}) at 37 °C in a 5% CO_2/95% air incubator in a humidified atmosphere, and culture media were replaced with fresh media two to three days. For fluorescence imaging, HeLa cells were grown in DMEM on a 35 mm glass bottom culture dishes for at least 24 h to enable adherence to the bottom.

The cells were loaded with **AZSiR** according to a following procedure. Briefly, the 50 μL of 100 μM **AZSiR** probes PBS solution was added to the dish (final concentration of **AZSiR** probes is 5 μM), and then the cells were incubated for 30 min at 37 °C. Afterward, the cells were washed several times with PBS for removing **AZSiR**. In CLSM imaging, the excitation wavelength was fixed at 635 nm and fluorescent signals were collected from 650 nm to 750 nm.

Acknowledgements

This work was supported by the National Natural Science Foundation of China (21274036), the Program for New Century Excellent Talents in University (NCET-12-0684), Training Program for Innovative Research Team and Leading talent in Hebei Province University (LJRC024). The Program for Innovative talent in Hebei Province University China (GCC2014054).

Notes and references

1 (*a*) E. Noelting and K. Dziewonsky, *Ber. Dtsch. Chem. Ges.*, 1905, **38**, 3516; (*b*) K. H. Drexhage, *J. Res. Natl. Bur. Stand., Sect. A*, 1976, **80**, 421; (*c*) K. H. Drexhage, *Laser Focus*, 1973, **9**, 35; (*d*) J. N. Demas and G. A. Crosby, *J. Phys. Chem.*, 1971, **75**, 991.

2 (*a*) I. S. Ioffe and V. F. Otten, *Zh. Obshch. Khim.*, 1961, **31**, 1511; (*b*) M. Beija, C. A. M. Afonsoa and J. M. G. Martinhoa, *Chem. Soc. Rev.*, 2009, **38**, 2410.

3 (*a*) W. Liu, M. Howarth, A. B. Greytak, Y. Zheng, D. G. Nocera, A. Y. Ting and M. G. Bawendi, *J. Am. Chem. Soc.*, 2008, **130**, 1274; (*b*) C. Hara, K. Tateyama, N. Akamatsu, H. Imabayashi, K. Karaki, N. Nomura, H. Okano and A. Miyawaki, *Brain Cell Biol.*, 2006, **35**, 229.

4 (*a*) L. Yuan, W. Lin, Y. Yang and H. Chen, *J. Am. Chem. Soc.*, 2012, **134**, 1200; (*b*) V. Grenier, A. S. Walker and E. W. Miller, *J. Am. Chem. Soc.*, 2015, **137**, 10894.

5 (*a*) M. S. T. Gonçalves, *Chem. Rev.*, 2009, **109**, 190; (*b*) J. Chan, S. C. Dodani and C. J. Chang, *Nat. Chem.*, 2012, **4**, 973.

6 (*a*) C. Tung, Y. Lin, W. Moon and R. Weissleder, *ChemBioChem*, 2002, **3**, 784; (*b*) R. Weissleder and V. Ntziachristos, *Nat. Med.*, 2003, **9**, 123; (*c*) K. Kiyose, H. Kojima and T. Nagano, *Chem.–Asian J.*, 2008, **3**, 506; (*d*) G. Qian and Z. Y. Wang, *Chem.–Asian J.*, 2010, **5**, 1006.

7 (*a*) J. V. Frangioni, *Curr. Opin. Chem. Biol.*, 2003, **7**, 626; (*b*) S. A. Hilderbrand and R. Weissleder, *Curr. Opin. Chem. Biol.*, 2010, **14**, 71; (*c*) L. Yuan, W. Lin, K. Zheng, L. He and W. Huang, *Chem. Soc. Rev.*, 2013, **42**, 622.

8 (*a*) M. Fu, Y. Xiao, X. Qian, D. Zhao and Y. Xu, *Chem. Commun.*, 2008, 1780; (*b*) Y. Koide, Y. Urano, K. Hanaoka, T. Terai and T. Nagano, *ACS Chem. Biol.*, 2011, **6**, 600; (*c*) T. Egawa, Y. Koide, K. Hanaoka, T. Komatsu, T. Teraiab and T. Nagano, *Chem. Commun.*, 2011, **47**, 4162; (*d*) B. Wang, X. Chai, W. Zhu, T. Wang and Q. Wu, *Chem. Commun.*, 2014, **50**, 14374; (*e*) Y. Kushida, T. Nagano and K. Hanaok, *Analyst*, 2015, **140**, 685.

9 (*a*) T. Egawa, K. Hirabayashi, Y. Koide, C. Kobayashi, N. Takahashi, T. Mineno, T. Terai, T. Ueno, T. Komatsu, Y. Ikegaya, N. Matsuki, T. Nagano and K. Hanaoka, *Angew. Chem., Int. Ed.*, 2013, **52**, 3874; (*b*) T. Myochin, K. Hanaoka, S. Iwaki, T. Ueno, T. Komatsu, T. Terai, T. Nagano and Y. Urano, *J. Am. Chem. Soc.*, 2015, **137**, 4759; (*c*) Y. Koide, Y. Urano, K. Hanaoka, W. Piao, M. Kusakabe, N. Saito, T. Terai, T. Okabe and T. Nag, *J. Am. Chem. Soc.*, 2012, **134**, 5029; (*d*) G. Lukinavicius, L. Reymond, K. Umezawa, O. Sallin, E. DEste, F. Göttfert, H. Ta, S. W. Hell, Y. Urano and K. Johnsson, *J. Am. Chem. Soc.*, 2016, **138**, 9365.

10 (*a*) T. Pastierik, P. Šebej, J. Medalova, P. Štacko and P. Klan, *J. Org. Chem.*, 2014, **79**, 3374; (*b*) Y. L. Huang, A. S. Walker and E. W. Miller, *J. Am. Chem. Soc.*, 2015, **137**, 10767; (*c*) J. B. Grimm, T. Klein, B. G. Kopek, G. Shtengel, H. F. Hess, M. Sauer and L. D. Lavis, *Angew. Chem., Int. Ed.*, 2016, **55**, 1723.

11 (*a*) J. B. Grimm, B. P. English, J. Chen, J. P. Slaughter, Z. Zhang, A. Revyakin, R. Patel, J. J. Macklin, D. Normanno, R. H. Singer, T. Lionnet and L. D. Lavis, *Nat. Methods*, 2015, **12**, 244; (*b*) V. Marx, *Nat. Methods*, 2015, **12**, 187.

12 (*a*) M. Kamiya, D. Asanuma, E. Kuranaga, A. Takeishi, M. Sakabe, M. Miura, T. Nagano and Y. Urano, *J. Am.*

Chem. Soc., 2011, **133**, 12960; (*b*) S. Uno, M. Kamiya, T. Yoshihara, K. Sugawara, K. Okabe, M. C. Tarhan, H. Fujita, T. Funatsu, Y. Okada, S. Tobita and Y. Urano, *Nat. Chem.*, 2014, **6**, 681; (*c*) G. Lukinavicius, K. Umezawa, N. Olivier, A. Honigmann, G. Yang, T. Plass, V. Mueller, L. Reymond, I. R. Correa Jr, Z. G. Luo, C. Schultz, E. A. Lemke, P. Heppenstall, C. Eggeling, S. Manley and K. Johnsson, *Nat. Chem.*, 2013, **5**, 132.

13 (*a*) X. Chen, T. Pradhan, F. Wang, J. S. Kim and J. Yoon, *Chem. Rev.*, 2012, **112**, 1910; (*b*) H. N. Kim, M. H. Lee, H. J. Kim, J. S. Kim and J. Yoon, *Chem. Soc. Rev.*, 2008, **37**, 1465.

14 (*a*) S. Choi, J. Bouffard and Y. Kim, *Chem. Sci.*, 2014, **5**, 751; (*b*) J. Wang, S. H. Zhong, W. F. Duan and B. X. Gao, *Tetrahedron Lett.*, 2015, **56**, 824.

15 Y. Urano, M. Kamiya, K. Kanda, T. Ueno, K. Hirose and T. Nagano, *J. Am. Chem. Soc.*, 2005, **127**, 4888.

16 (*a*) B. X. Gao, H. X. Li, H. M. Liu, L. C. Zhang, Q. Q. Bai and X. W. Ba, *Chem. Commun.*, 2011, **47**, 3894; (*b*) H. M. Liu, L. Y. Wang, C. H. Liu, H. X. Li, B. X. Gao, L. C. Zhang, F. L. Bo, Q. Q. Bai and X. W. Ba, *J. Mater. Chem.*, 2012, **22**, 6176.

17 (*a*) E. E. Neuteboom, S. C. J. Meskers, E. W. Meijer and R. A. J. Janssen, *Macromol. Chem. Phys.*, 2004, **205**, 217; (*b*) K. R. Wang, Z. B. Yang and X. L. Li, *Chem.–Eur. J.*, 2015, **21**, 5680.

18 (*a*) R. P. Haugland, *The Handbook: A Guide to Fluorescent Probes and Labeling Technologies*, Invitrogen, Eugene, OR, 10th edn, 2005; (*b*) C. Kohl, T. Weil, J. Qu and K. Müllen, *Chem.–Eur. J.*, 2004, **10**, 5297; (*c*) L. B. Bai, W. Li, J. T. Chen, F. L. Bo, B. X. Gao, H. M. Liu, J. J. Li, Y. G. Wu and X. W. Ba, *Macromol. Rapid Commun.*, 2013, **34**, 539; (*d*) X. H. Li, X. H. Gao, W. Shi and H. M. Ma, *Chem. Rev.*, 2014, **114**, 590.

19 Z. H. Lei, X. R. Li, Y. Li, X. Luo, M. M. Zhou and Y. J. Yang, *J. Org. Chem.*, 2015, **80**, 11538.